

# Development and characterization of a ZnO/Ge photodiode for optical radiation measurements in the near infrared

Zahra Ben Achour<sup>1,\*</sup>, Marwa Hammami<sup>2</sup>, and Oualid Touayar<sup>1</sup>

<sup>1</sup> Metrology Team of Radiometric and Pyrometric Measurements, Carthage University, National Institute of Applied Science and Technology, INSAT BP676 Centre Urbain Nord, 1080 Tunis Cedex, Tunisia

<sup>2</sup> University Campus Farhat Hachad, Tunis, El Manar University, Faculty of Sciences of Tunis, Tunis, Tunisia

Received: 19 December 2016 / Accepted: 2 May 2017

**Abstract.** The metrology group of radiometric and pyrometric measurements of INSAT include among others the development of detectors that will be used as a standard in the MMA Laboratory for optical radiation measurements in the visible and infrared spectral range. In this work, we present the design and realization of a detector for near infrared radiation measurements: it is a photodiode ZnO/Ge based on a germanium junction and a thin layer of zinc oxide. Then we electrically and optically characterized the photodiode thus realized, for which we developed an energy band diagram. The obtained results have allowed us to note an improvement in the optical and electrical characteristics of the ZnO/Ge photodiode, compared to those performed in our laboratory and based on single Germanium. The reflectivity is reduced by about 9% for the wavelength range of 800 nm to 2000 nm. The shunt resistance increases from 95  $\Omega$  to 12.915 k $\Omega$ . However, the series resistance increases from 1.08  $\Omega$  to 36  $\Omega$  but it is still an acceptable value. The proposed energy band diagram explains the charge carrier transport phenomena for our structure and it is in good agreement with experimental results.

**Keywords:** photodiode / zinc oxide / transfer detector / reflectivity / radiometric measurements

## 1 Introduction

Research work carried out within the metrology group of radiometric and pyrometric measurements of INSAT, have achieved NP junctions by ion implantation from Ge p-type substrate and the realization of porous germanium photodiodes [1–3]. These studies have shown an improvement in the absorption of the incident light with respect to the commercial photodiodes based on the junction germanium.

The only devices to minimize the reflection coefficient are trap detectors requiring the use of several photodiodes placed in well-defined geometric configurations (3–5 photodiodes). Our objective is to realize a detector with a low reflection coefficient using a single photodiode, hence the interest of optical characterization.

In the current work, we study the influence of a thin ZnO layer deposited onto a Ge junction. Indeed, the ZnO thin films in addition to their transparent features in the near infrared, are excellent candidates for the transparent electrodes and antireflective coats [3–5]. The optical and electrical properties of ZnO thin films allow them to reduce

the reflectivity of the substrates on which they are deposited and to drive the charges created on the surface to the outer circuit [6].

The spectral sensibility of the photodiodes is proportional to the reflexion coefficient and the internal quantum efficiency (Eq. (1)) which itself depends on the diffusion constant of the charge carriers in the semiconductors [1,6].

$$S = e\eta(1 - \rho) \frac{\lambda}{hc}, \quad (1)$$

with  $\rho$ : reflexion coefficient;  $\eta$ : internal quantum efficiency;  $\lambda$ : wave length;  $h$ : Planck constant;  $c$ : light speed;  $e$ : electron charge.

The improvement of the spectral sensitivity is achieved by reducing the reflection coefficient and by increasing the internal quantum efficiency varying in the same way as the diffusion constant of the semiconductor.

In order to have a large diffusion constant, it is necessary to have a low recombination rate of the charge carriers. This is ensured only by low series resistance and high shunt resistance.

In order to evaluate the quality of our photodiodes, we will proceed to their electrical characterization. This will allow us to evaluate the different electrical characteristics

\* Corresponding author: [zbenachour@yahoo.fr](mailto:zbenachour@yahoo.fr)

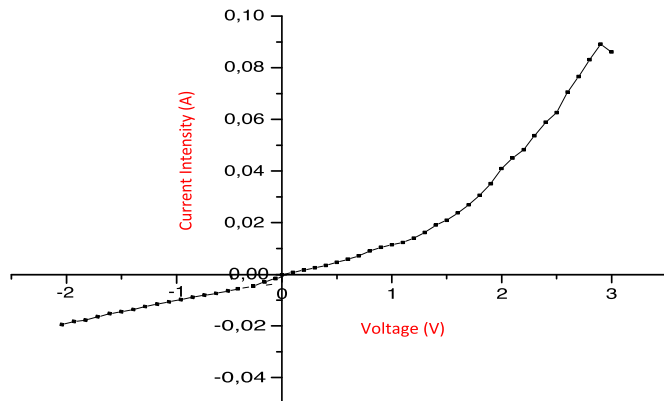


**Fig. 1.**  $I$ - $V$  characteristic of the germanium junctions.

of our devices and the direction of their evolution in order to compare them with commercially available standard photodiodes.

In the first part of this paper we present the results of electrical and optical characterization of germanium junctions.

In the second part we are interested in the characterization of the new photodiode type ZnO/Ge that we developed. These photodiodes are Germanium junctions formed by ion implantation where we deposited on the front face a thin layer of zinc oxide by the Spray pyrolysis technique [4,7,8].

## 2 NP germanium junctions characterization

The used NP germanium junctions are made by ion implantation from germanium polymer substrate type P. This P-type substrate is initially doped gallium with (1,0,0) orientation, a resistivity lower than  $1 \Omega \text{ cm}$  and a thickness of  $300 \mu\text{m}$ . These substrates have a reflectivity of about 33% for the wavelength range between 800 nm and 2000 nm [1,2]. Ion implantation is performed by the ion implanter installed in Microelectronics Institute of Barcelona in Spain. It is performed with an ionizing beam energy of 150 keV for phosphorus impurity doses of  $1 \times 10^{-15} \text{ atm/cm}^2$  [1,9,10]. The realized junctions have a junction depth of about  $0.4 \mu\text{m}$ . The metallic contacts are made by thermal evaporation, with gold covering the entire backside and gold circle electrode on the front side of the junctions.

### 2.1 Electrical characterization of germanium junctions

The  $I$ - $V$  characteristic shows the internal processes that regulate the operation of the photodiode. It also represents the macroscopic characteristics  $R_s$ ,  $R_{sh}$ ,  $I_{ph}$  and the current diodic showing the transport phenomena of the charge carriers within the structure. The series resistance  $R_s$  of a photodiode arises from the resistance of the contacts and the resistance of the undepleted germanium. It therefore models the carriers transport in the depletion zone. As for the shunt resistance  $R_{sh}$ , it models the current leakage and charge carriers in the depletion zone. The  $I_{ph}$  is the photonic current of the photodiode.

**Table 1.** Electrical parameters of germanium junctions.

Threshold voltage, $V_s$	0.411 V
Photonic current, $I_{ph}$	$-8.52 \times 10^{-5} \text{ A}$
Saturation current, $I_{sat}$	$1.06 \times 10^{-4} \text{ A}$
Series resistance, $R_s$	1.08
Shunt resistance, $R_{sh}$	94.98

The  $I$ - $V$  characteristic in darkness is detected on a measurement bench where the photodiode are biased by a voltage supplied by a DC power supply.

The method of determining the electrical parameters of the photodiode has been widely detailed in several publications [1,11]. This method is based on the tracing of the corresponding characteristics  $\text{Ln}(I) = f(V)$  from the experimental responses  $I$ - $V$ . The advantage of studying the characteristics  $\text{Ln}(I) = f(V)$  is to show efficiently the different modes of conduction, to be able to localize them according to the voltage and to determine approximately the saturation current and the series and shunt resistances.

According to the  $I$ - $V$  characteristic curve in Figure 1, we deduce the photonic current corresponding to our germanium junctions. Exploiting this characteristic also allowed us to determine the values of the series resistance and the shunt resistance. Table 1 was synthesized various electrical parameters of the germanium junctions.

The series resistance is similar to those of commercial photodiodes of few ohms. The series resistance low value of our device, highlights the quality of the internal structure. Indeed, the ion implantation is a doping process that results in a uniform distribution of implanted impurities. Furthermore, the post-implantation treatment can cure defects appeared during implantation which reduced the traps of the charge carriers and thus the series resistance.

The shunt resistance of the junctions is lower than that of available commercial photodiodes which have a shunt resistance of a few hundred kilo ohms. Indeed, this resistance characterizes losses by recombination of the carriers due to the germanium structural defects. The existence of cracks and structural complex defects in surface becomes the seat of physical phenomenon similar to a parallel resistor  $R_{sh}$  [9,10].

### 2.2 Optical characterization of the germanium junctions

The reflectivity determination allows us to evaluate the level of reflection loss of the incident luminous flux on the Ge/Air interface of the device forming the photodiode. The measurements were performed at the Laboratory of Physics Condensed Matter (LPMC) of the Faculty of Sciences of Tunis with a spectrophotometer Perkin Elmer Lambda 950. The spectral range extended from 200 nm to 2500 nm.

Figure 2 represents the results of the reflectivity measured on the photodiodes based on germanium junction.

The reflectivity of germanium junctions is about 30% within the wavelength range from 800 nm to 2000 nm. We note also a slight reduction in the reflectivity of around 3% between germanium junctions and the base bare germani-

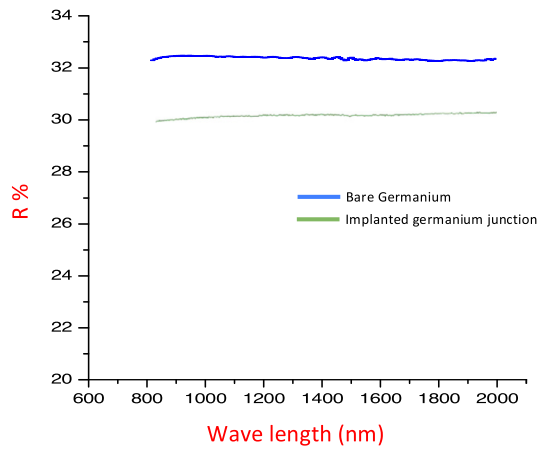


Fig. 2. Reflectivity of germanium junctions.

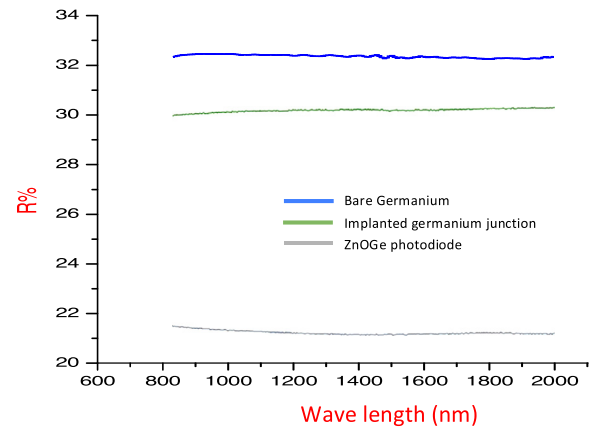


Fig. 4. Reflectivity of the ZnO/Ge photodiode.

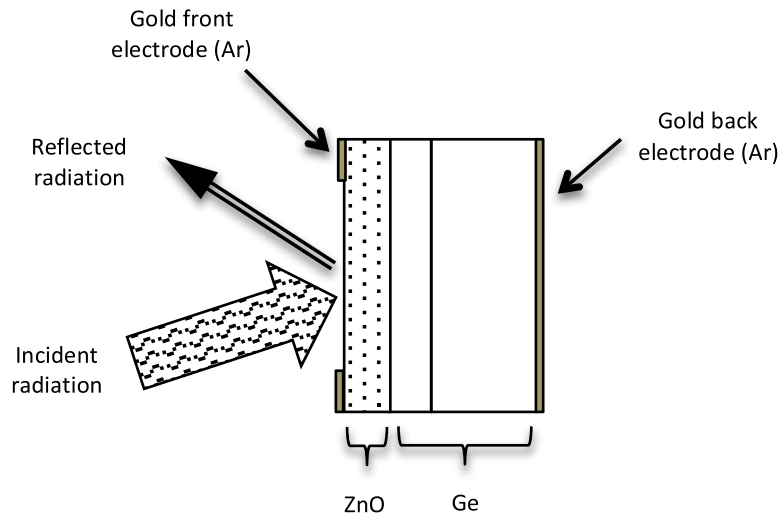


Fig. 3. Structure of the ZnO/Ge photodiode.

um. This reflectivity reduction is partly due to the native oxide on the surface of the germanium substrate, in addition to the oxidation of germanium during the post-implantation treatment. Indeed, ion implantation generates a crystallographic disorder at the implanted matrix, thereby requiring an annealing which will cure the defects induced by implantation to activate the implanted impurities and homogenize the doped layer. The analysis of results allows us to deduce that after optimization of manufacturing conditions of the junctions, it is imperative to introduce antireflection layers in the structure of germanium photodiodes to reduce reflectivity. These layers enable to reduce the reflectivity and in the other hand chemically stabilize the surface of the germanium and preserve its physical and chemical characteristics.

### 3 ZnO deposition on Ge junctions: optical and electrical characterization

The ZnO thin films are deposited by spray pyrolysis technical in inert atmosphere from a 0.1 M zinc acetate solution 3% doped with aluminum. The deposition

temperature is 460 °C for optimal duration of 60 min [4]. The choice of this temperature allows to obtain 90% transparent ZnO layers in the range of 500–2500 nm. The ZnO thin films thus produced have a resistivity of  $3 \times 10^{-3} \Omega \text{ cm}$  and a preferred crystallographic orientation (0,0,2) [4]. The thickness of these thin films is approximately 1  $\mu\text{m}$  and their gaps is of the order of 3.21 eV [4]. Figure 3 shows a section of the structure forming the achieved ZnO/Ge photodiode.

#### 3.1 Optical characterization of the ZnO/Ge structure

We are interested in this part to the study of the reflectivity in the spectral range from 800 to 2000 nm, of the new structure the ZnO/Ge photodiode. The results of this study made on the same spectrometer previously used (Sect. 2.2), are represented in Figure 4.

We find that the ZnO layers bring a reduction in the reflectivity of Ge junctions. In fact, the reflectivity passes from an average value of 30–21% over a wavelength range between 800 and 2000 nm which is therefore a gain of about 9% for the light absorption. This gain is due to the antireflective feature of the ZnO thin films deposited on the

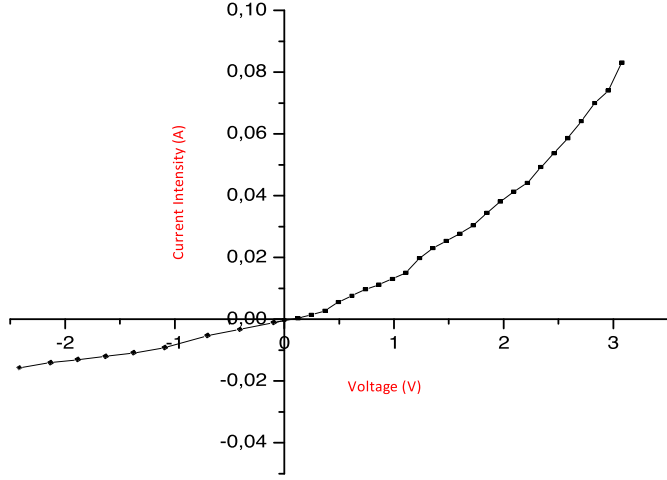


Fig. 5.  $I$ - $V$  characteristic of the ZnO/Ge photodiode.

germanium junction. Indeed, it has been demonstrated that the thin layers of ZnO thus deposited have a reflectivity level on average equal to 20% in the spectral range from 400 to 1800 nm [4].

### 3.2 Electrical characterization of the ZnO/Ge structure

For this part we have adopted the same approach described above. Figure 5 we represent the  $I$ - $V$  characteristic of the ZnO/Ge photodiode.

According to this graph, it can be deduced that the structure of the germanium photodiode covered with a thin ZnO layer on its front face, has a series resistance  $R_s$  and a shunt resistance  $R_{sh}$ , higher than the photodiode formed by a germanium bare junction. Indeed, the slope  $\Delta I/\Delta V$  ( $V \rightarrow 0$ ) decreases significantly, resulting in a decrease in leakage current and a significant increase in the shunt resistance.

The characteristic parameters of the ZnO/Ge photodiode are summarized in Table 2.

When the germanium photodiode is provided with a thin layer of ZnO, there is a clear improvement in its current response following the change in voltage which reflects the new values of shunt and series resistances we could get.

The improvement of the  $I$ - $V$  characteristic after introduction of the ZnO layer in the photodiode structure is due to the optical and electrical characteristics of this layer. Indeed, the antireflection appearance of the ZnO layer contributed to the optic flux confinement which improves the absorption of the photodiode and hence its response. The photonic current determined from the  $I$ - $V$  characteristic under illumination is in the order of  $-1.22 \times 10^{-5}$  A.

The considerable increase in the shunt resistance from  $94.98 \Omega$  to  $12.915 \text{ k}\Omega$  after the thin ZnO layer deposition is due to the passivation of dangling bonds of the germanium as well as the native oxide. This therefore leads to a reduction of the quantum wells as well as of imperfections where the charge carriers are trapped especially in surface. Besides, the ZnO thin films are transparent electrodes that

Table 2. Electrical parameters of the ZnO/Ge photodiode.

Threshold voltage, $V_s$	0.471 V
Photonic current, $I_{ph}$	$-1.22 \times 10^{-5}$ A
Saturation current, $I_{sat}$	$1.8 \times 10^{-4}$ A
Series resistance, $R_s$	36
Shunt resistance, $R_{sh}$	12.915 k

recover the charges created on the surface. This has the effect of reducing the recombination velocity of charge carriers and to extend their lifetime in surface.

Furthermore, there is an increase of the series resistance which characterizes the internal resistance. The series resistance changes from a value of  $1.08 \text{--} 36 \Omega$ . This variation is probably due to the thermal agitation effects on the internal structure of the junction after annealing during deposition of the ZnO layer. We can also attribute this increase in the potential barrier that is created at the interface between ZnO layer and the germanium surface. Indeed, the gap of germanium is 0.66 eV [1] and that of the deposited ZnO layer is of the order of 3.21 eV [4].

## 4 Energy bands diagram

To understand the conversion process of the charge carriers and explain the improvement made by depositing ZnO thin films on germanium photodiodes, we propose a diagram of the energy bands of the ZnO/Ge structure thus formed. The physical model of the energy bands diagram that we propose is a model explaining the mechanisms of electrical conduction within our photodiode and it takes into account the different layers and their physical properties.

Our studied structure is a heterojunction in which two different types of semiconductor are brought into contact. Therefore they exchange electrons so as to align their Fermi levels. This exchange takes place near the junction thereby creating a space charge zone which is associated with a potential barrier  $V_d$  which stops the carrier diffusion and defines the state of equilibrium.

$$V_d = V_2 - V_1 = \phi_1 - \phi_2, \quad (2)$$

where  $V_1$  and  $V_2$ : potentials of the two semiconductors and  $e\phi_1$ ,  $e\phi_2$ : the corresponding output works.

The condition  $\phi_2 > \phi_1$  leads  $V_d < 0$ , and it establishes a positive potential difference between the semiconductor with low work function and the semiconductor with high work function.

The differences in density of states and semiconductor doping carry different values of the parameters  $e\phi_{F_1}$  and  $e\phi_{F_2}$ , so different values of the conduction bands energies of the two neutral regions of the semiconductors that is [12]:

$$\Delta E_{c_n} = \Delta E_{c_1} - \Delta E_{c_2} = e(\phi_{F_1} - \phi_{F_2}), \quad (3)$$

where  $e\phi_{F_1} = E_{c_1} - E_{F_1}$  and  $e\phi_{F_2} = E_{c_2} - E_{F_2}$  with  $\Delta E_{c_n}$ : the energy difference of the conduction bands;  $\Delta E_{v_n}$ : the energy difference of the valence bands;  $\Delta E_g$ : the gaps

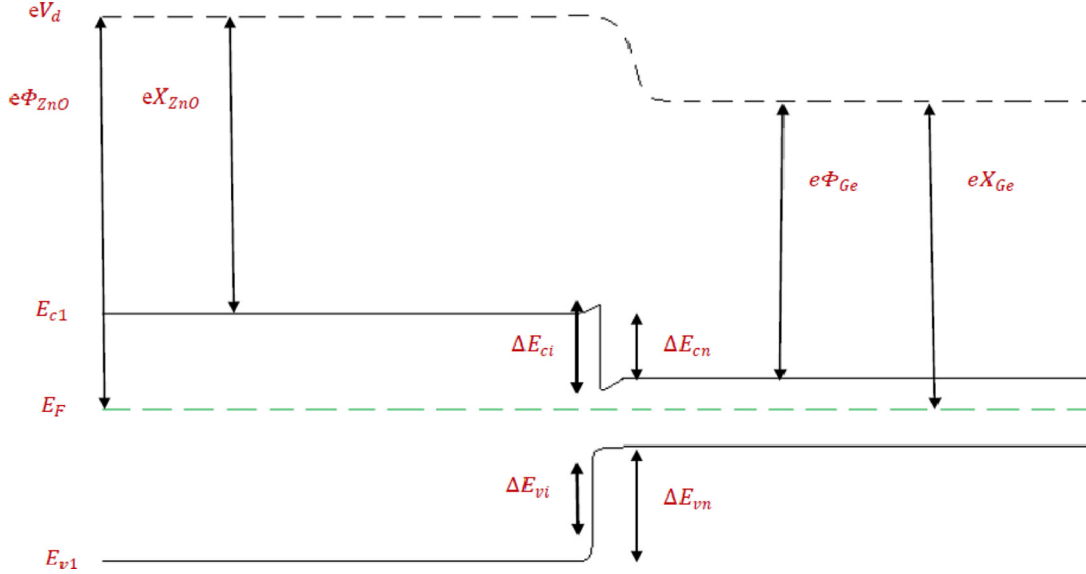


Fig. 6. Diagram of energy bands structure of ZnO/n-type germanium.

difference of the two semiconductors;  $E_{c_i}$ : the conduction band energies of the semiconductor  $i$  ( $i = 1; 2$ );  $E_{F_i}$ : the fermi energies of the semiconductor  $i$  ( $i = 1; 2$ ).

Finally, if the gap difference of the energies of the two semiconductors is different from  $\Delta E_{c_n}$ , the complement is expressed by an energy difference  $E_g$  between the valence bands and the conduction bands:

$$\Delta E_g = E_{g_2} - E_{g_1} = (E_{c_2} - E_{c_1}) - (E_{v_2} - E_{v_1}),$$

$$\text{So : } \Delta E_g = \Delta E_{c_n} - \Delta E_{v_n}, \quad (4)$$

with  $\Delta E_{v_n}$ : the energy difference of the valence bands;  $\Delta E_g$ : the gaps difference of the two semiconductors.

The energy difference of the valence bands is therefore given by:

$$\Delta E_{v_n} = e(\phi_{F_2} - \phi_{F_1}) - \Delta E_g.$$

Moreover

$$\begin{aligned} \Delta E_{c_n} &= e(\phi_{F_2} - \phi_{F_1}) = e[(\phi_2 - \chi_2) - (\phi_1 - \chi_1)] \\ &= -eV_d - e(\chi_2 - \chi_1), \end{aligned} \quad (5)$$

$$\text{So : } \Delta E_{v_n} = -eV_d - [e(\chi_2 - \chi_1) + \Delta E_g], \quad (6)$$

with  $e\chi_1$ : the electronic affinity of the semiconductor 1;  $e\chi_2$ : the electronic affinity of the semiconductor 2.

Due to the continuity of the potential at the interface  $V_1 = V_2$  and therefore the equations 4 and 5 become in the vicinity of the junction:

$$\Delta E_{c_n}(\text{at the interface}) = -e(\chi_2 - \chi_1), \quad (7)$$

$$\Delta E_{v_n}(\text{at the interface}) = -[e(\chi_2 - \chi_1) + \Delta E_g]. \quad (8)$$

#### 4.1 Heterojunction n-n: zinc oxide-germanium

Our hetero structure corresponds to a junction of zinc oxide on the n-type front of a poly-mirror germanium photodiode where  $e\phi_{ZnO} > e\phi_{Ge}$ .

Thus, the electrons diffuse from the germanium to the zinc oxide and the holes from the zinc oxide to the germanium. The state of equilibrium is established by diffusion so the electrons are repelled from the interface and the holes are drawn.

We have:  $E_{ZnO} = 3.33 \text{ eV}$  [4],  $e\chi_{ZnO} = 4.1 \text{ eV}$  [12],  $e\phi_{ZnO} = 5.33 \text{ eV}$  [13],  $E_{Ge} = 0.66 \text{ eV}$  [13],  $e\chi_{Ge} = 4 \text{ eV}$  [14],  $e\phi_{Ge} = 4.16 \text{ eV}$  [14].

When  $eV_d = e(V_2 - V_1) = -(e\phi_{Ge} - e\phi_{ZnO}) = -1.17 \text{ eV}$ .

In the vicinity of the junction we have:

$$-e(\chi_{Ge} - \chi_{ZnO}) = 0.1 \text{ eV},$$

$$\Delta E_g = E_{Ge} - E_{ZnO} = -2.67 \text{ eV},$$

$$-[\Delta E_g + e(\chi_{Ge} - \chi_{ZnO})] = 2.77 \text{ eV}.$$

Therefore

$$\Delta E_{c_n} = -[e(\phi_{Ge} - \phi_{ZnO}) - e(\chi_{Ge} - \chi_{ZnO})] = -1.27 \text{ eV},$$

$$\Delta E_{v_n} = -[\Delta E_g + e(\chi_{Ge} - \chi_{ZnO})] - eV_d = 3.94 \text{ eV}.$$

From the various explanations, we can propose as an energy diagram of the first part of our designed structure so ZnO/front germanium photodiode, the following diagram (Fig. 6).

Following the diffusion of electrons from Ge to ZnO and holes from ZnO to Ge, it appears a positive space charge zone in the Ge and a negative one in ZnO. The nature and extent of the space charge zone depends on the type of each semiconductor.

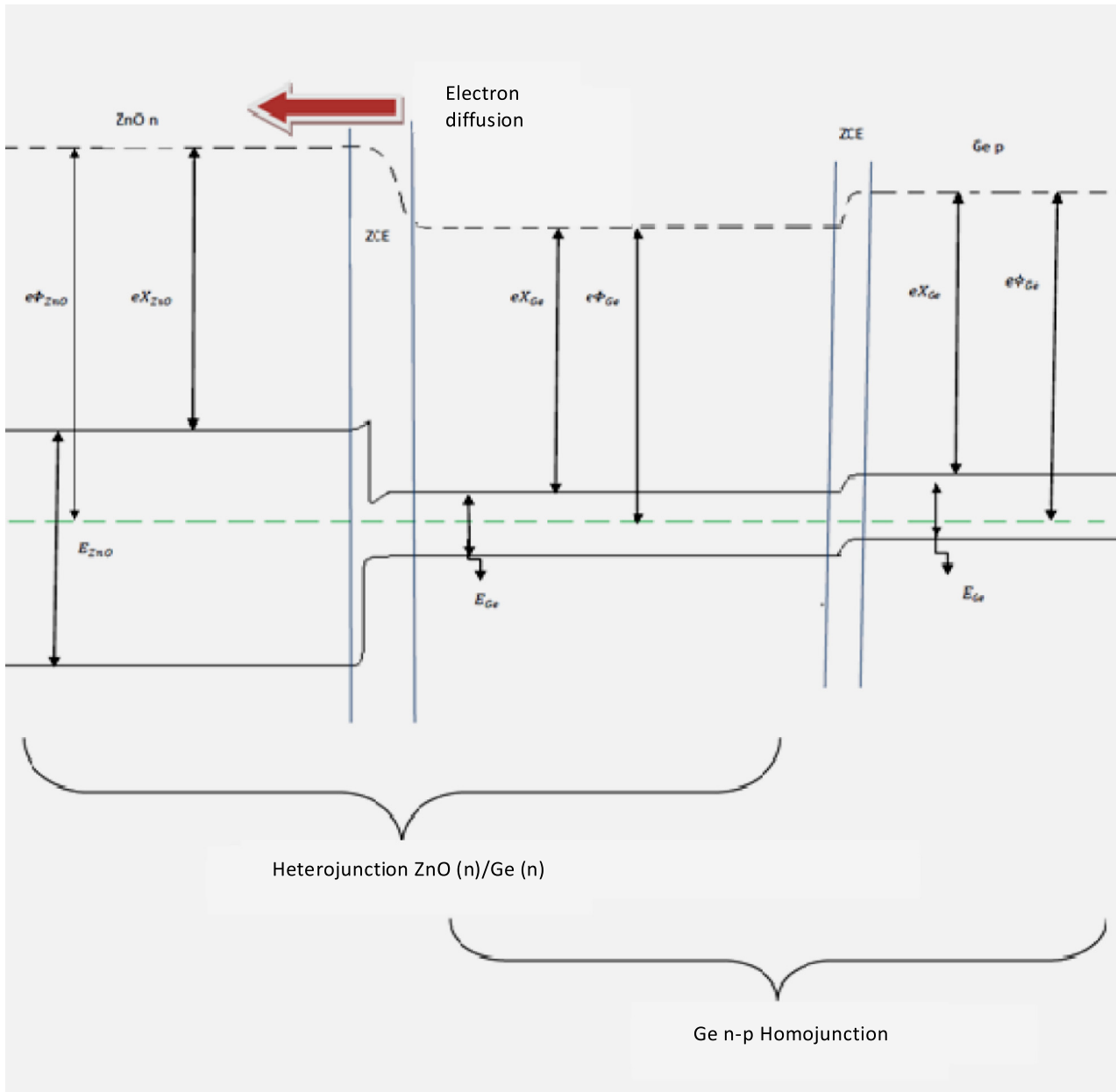


Fig. 7. Energy band diagram of the entire ZnO/Ge photodiode.

In the ZnO semiconductor the space charge zone is negative. It is due to an increase in electron density in the vicinity of the interface. Hence the space charge in the ZnO semiconductor is an accumulating charge and it is located in the immediate vicinity of the interface. For the Ge semiconductor the space charge zone is at contrary positive. It is established in the vicinity of the interface a depletion regime with a certain spatial extension of the charge density.

#### 4.2 Final diagram of the ZnO/Ge photodiode

The structure of our ZnO/Ge photodiode consists of two parts. The first part is an heterojunction n-n zinc oxide and germanium. The second part is a n-p homojunction germanium which formed the basis of photodiode before the deposition of the ZnO layer.

Taking into account all the characteristic parameters of all parts of the ZnO/Ge photodiode, we propose in Figure 7 an energy bands diagram of the structure.

The current is still more important at a strong discontinuity than at the level of a pseudo-continuity. Near to the strong discontinuity, the potential barrier is relatively low near the top so some carriers can pass through it by Tunnel effect. This process can be described by an intra-band process [12].

## 5 Conclusion

The electrical and optical studies on the ZnO/Ge photodiode, demonstrate the significant improvement of germanium junctions after introduction of thin aluminum-

doped ZnO layers in the structure. Indeed, we have noted a reduction in the reflectivity of 13%. The new photodiode has a reflectivity of some 21% on average over the wavelength range of 800–2000 nm. We also highlighted the improvement of the electrical characteristics particularly the shunt resistance which climbed from  $95\ \Omega$  up to  $12.915\ \text{k}\Omega$  with the deposit of the thin ZnO layer. Nevertheless we have noted a slight increase in the series resistance, which rose from  $1.08\ \Omega$  to  $36\ \Omega$  but still comparable to the commercial photodiodes. The proposed energy band diagram explains the transfer process of carriers charge in the different sections of our ZnO/Ge structure. It also brings some additional physical arguments to the observed electrical improvements. We plan to further work in order to lead a metrological study of the performed photodiode. This will eventually help to design this type of photodiode for radiometric applications in our metrology laboratory.

## References

1. E. Akkari, O. Touayar, F.J. del Campo, J. Monteserrat, Improved electrical characteristics of porous germanium photodiode obtained by phosphorus ion implantation, *Int. J. Nanotechnol.* **10**, 553–562 (2013)
2. E. Akkari, Z. Ben Achour, S. Aouida, O. Touayar, B. Bessais, J. Ben Brahim, Study and characterization of porous germanium for radiometric measurements, *Phys. Status Solidi C* **6**, 1685–1688 (2009)
3. E. Akkari, O. Touayar, B. Bessais, Reflectivity, absorption and structural studies of porous germanium, *Sensor Lett.* **9**, 2295–2298 (2011)
4. Z. Ben Achour, T. Ktari, B. Ouertani, O. Touayar, B. Bessais, J. Ben Brahim, Effect of doping level and spray time on zinc oxide thin films produced by spray pyrolysis for transparent electrodes applications, *Sens. Actuators A* **134**, 447–451 (2007)
5. S. Major, S. Kumar, M. Bhatnagar, *Appl. Phys. Lett.* **49**, 394 (1986)
6. Z. Ben Achour, O. Touayar, E. Akkari, J. Bastie, B. Bessais, J. Ben Brahim, Study and realization of a transfer detector based on porous silicon for radiometric measurements, *Nucl. Instrum. Methods Phys. Res. A* **579**, 1117–1121 (2007)
7. F. Paraguay, W. Estrada, D.R. Acosta, *Thin Solid Films* **350**, 192 (1999)
8. M. Amlouk, F. Touhari, S. Belgacem, N. Kamoun, R. Bennaceur, *Phys. Status Solidi (a)* **163**, 73 (1997)
9. E. Simoen, A. Satta, A. D'Amore, T. Janssens, T. Clarysse, K. Martens, B. De Jaeger, A. Benedetti, I. Hoflijk, B. Borijs, M. Meuris, W. Vandercost, *Mater. Sci. Semicond. Process.* **9**, 634–639 (2006)
10. Th. Canneaux, D. Mathiot, J.P. Ponpon, S. Roques, S. Schmitt, Ch. Dubois, *Mater. Sci. Eng. B* **154–155**, 68–71 (2008)
11. Z. Ben Achour, O. Touayar, N. Sifi, Stability study of the metrological characteristics of a ZnO/PS/C-Si photodiode (PSiZ) used as a transfer standard in the visible spectral range, *Mod. Instrum.* **1**, 21–25 (2012)
12. H. Mathieu, *Physique des semi-conducteurs et des composants électronique* (Edition Masson, 2009), pp. 300–334
13. S.Yu. Davydov, V.A. Moshnikov, A.A. Fedotov, Gas adsorption on semiconducting oxides: a change in the work function, *Tech. Phys. Lett.* **30**, 727–729 (2004)
14. Handbook of semiconductor germanium technology/germanium based from materials to devices, Vol. 4, 2nd edition, *Methods A* **518**, 775 (2004)

**Cite this article as :** Zahra Ben Achour, Marwa Hammami, Oualid Touayar, Development and characterization of a ZnO/Ge photodiode for optical radiation measurements in the near infrared, *Int. J. Metrol. Qual. Eng.* **8**, 24 (2017)